

Unconventional superconductivity in $\text{YNi}_2\text{B}_2\text{C}$

T. R. Abu Alrub and S. H. Curnoe

*Department of Physics and Physical Oceanography,
Memorial University of Newfoundland, St. John's, NL, A1B 3X7, Canada*

We use the semi-classical (Doppler shift) approximation to calculate magnetic field angle-dependent density of states and thermal conductivity κ_{zz} for a superconductor with a quasi-two-dimensional Fermi surface and line nodes along $k_x = 0$ and $k_y = 0$. The results are shown to be in good quantitative agreement with experimental results obtained for $\text{YNi}_2\text{B}_2\text{C}$ (Ref. 1).

PACS numbers: 74.20.-z, 74.20.Rp, 74.25.Fy, 74.70.Dd

I. INTRODUCTION

$\text{YNi}_2\text{B}_2\text{C}$ is a type II superconductor with a relatively high transition temperature $T_c = 15.6\text{K}$.² Although initially thought to be a conventional s -wave superconductor, accumulated evidence soon suggested otherwise. Power law behaviour in the heat capacity $C_p/T \propto T^2$ was the first indication that $\text{YNi}_2\text{B}_2\text{C}$ is an unconventional superconductor with point nodes in the gap function.^{3,4} However, the field dependence of the heat capacity was found to be $C_p \propto \sqrt{H}$, indicative of line nodes.^{4,5} The NMR spin relaxation rate $1/T_1$ was measured to be $\propto T^3$ with no Hebel-Slichter peak⁶, again consistent with line nodes in the gap function. Finally, Raman scattering showed a peak in the electronic A_{1g} and B_{2g} response,⁷ possibly indicative of a B_{2g} symmetry gap function. Such a gap function takes the form $\Delta(\mathbf{k}) \propto k_x k_y$, and thus has symmetry required line nodes along $k_x = 0$ and $k_y = 0$.^{8,9} In contrast to these findings, field-angle dependent measurements of thermal conductivity and specific heat were claimed to be indicative of point nodes in the gap function.^{1,10,11} The reconciliation of these results, and hence the symmetry of the gap function, remains an important unresolved issue.

$\text{YNi}_2\text{B}_2\text{C}$ belongs to the crystallographic space group $I4/mmm$ (No. 139, D_{4h}^{17}).¹² The lattice is body-centred tetragonal (bct) with $a = 3.526\text{\AA}$ and $c = 10.543\text{\AA}$.³ According to symmetry analysis for D_{4h} crystals,^{8,9} gap functions with line nodes are found only for singlet pairing, while point nodes are found only for triplet pairing. Various nodal configurations can occur, depending on the irreducible representation of D_{4h} by which the superconducting order parameter transforms. Nodes in the gap function are normally detected via quasiparticles (q.p.'s) which appear in the vicinity of gap nodes in k -space as a result of either finite temperature, impurities, or Doppler shift in the presence of an applied magnetic field. In these kinds of measurements, the nodes will be invisible if there is no Fermi surface in the direction of the nodes, thus the shape and connectivity of the Fermi surface plays an important role.

The Fermi level crosses the 17th, 18th and 19th bands. The topology of the Fermi surface is highly sensitive to the precise position of the Fermi level due to a dispersionless band between the Γ and X points. Thus

different band structure calculations share common features but the resulting Fermi surfaces have significant differences.^{13,14,15} Yamaguchi et al.¹⁵ correlated their results with de Haas-van Alphen (dHvA) measurements in order to fix the Fermi energy. The 18th and 19th bands were found to produce closed Fermi surfaces around various points in the Brillouin zone, however the 17th band produces a large electron Fermi surface multiply connected by necks. Part of this surface appears as dHvA oscillations perpendicular to the c -axis. The orbits do not appear to be closed in the c direction; instead they seem to possess a two-dimensional character that extends in the c direction, as evidenced by the upward curvature of the dHvA frequencies about the $[001]$ direction, shown in Fig. 3 of Ref. 15.

In the vortex phase of a type II superconductor q.p.'s may be either *localised* about vortex cores or *delocalised*. It was shown some time ago that the contribution to the low-energy density of states in a superconductor with line nodes comes from *delocalised q.p.'s in the vicinity of the nodes*.¹⁶ The delocalised q.p.'s can be treated with a semi-classical (Doppler shift) approximation; this approach provided a good description of field-dependent specific heat and thermal conductivity of the line node superconductors $\text{YBa}_2\text{Cu}_3\text{O}$ [17] and CeCoIn_5 [5]. However, Volovik's argument does not extend to point node superconductors. For point node superconductors, the semi-classical calculation may still be performed,¹⁸ but, as may be expected, these results are not in agreement with any experiment involving putative point node superconductors so far.

In this article, we use the semi-classical approximation to calculate the field-angle dependent density of states and thermal conductivity for a superconductor with line nodes and a quasi-2D Fermi surface, for the purpose of demonstrating that the results of such measurements on $\text{YNi}_2\text{B}_2\text{C}$ are in fact consistent with this scenario, in contrast to what has been claimed.¹

For simplicity, we assume that the Fermi surface has the shape shown in Fig. 1, for which the q.p. energy spectrum takes the form

$$\varepsilon(\mathbf{k}) = \frac{k_x^2 + k_y^2}{2m} + \varepsilon'_F \cos ck_z - \varepsilon_F \quad (1)$$

where $\varepsilon'_F \equiv \frac{k'_F c}{2m} \ll \varepsilon_F$. A gap function with B_{2g} sym-

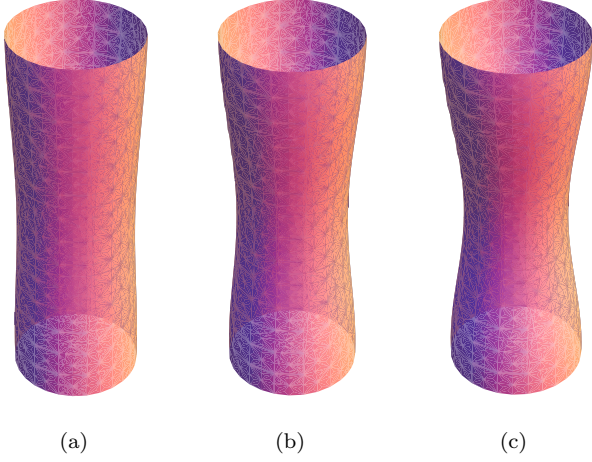


FIG. 1: (Colour online) Fermi surfaces for three different values of $b = \frac{v'_F}{v_F}$. The surface in c) has the largest value of b .

metry has line nodes along $k_x = 0$ and $k_y = 0$. The Fermi momenta along these nodes (parametrised by k_z) are

$$\begin{aligned} \mathbf{k}_{F1,3} &= (0, \pm(2m(\varepsilon_F - \varepsilon'_F \cos ck_z))^{1/2}, k'_F \sin ck_z) \\ &\approx (0, \pm k_F, k'_F \sin ck_z) \end{aligned} \quad (2)$$

$$\begin{aligned} \mathbf{k}_{F2,4} &= (\pm(2m(\varepsilon_F - \varepsilon'_F \cos ck_z))^{1/2}, 0, k'_F \sin ck_z) \\ &\approx (\pm k_F, 0, k'_F \sin ck_z). \end{aligned} \quad (3)$$

The magnetic field rotates in the xy plane with an angle ϵ with respect to the x axis,

$$\mathbf{H} = H(\cos \epsilon, \sin \epsilon, 0). \quad (4)$$

The supercurrent circulates perpendicular to the field as a function of the distance r from the vortex core and winding angle β ,

$$\mathbf{v}_s(\mathbf{r}) = \frac{1}{2mr}(-\sin \epsilon \cos \beta, \cos \epsilon \cos \beta, \sin \beta). \quad (5)$$

The Doppler shifts associated with each line node are $\alpha_i(\mathbf{r}) = \mathbf{k}_{Fi} \cdot \mathbf{v}_s$,

$$\alpha_{1,3}(\mathbf{r}) = \frac{1}{2mr}[\pm k_F \cos \epsilon \cos \beta + k'_F \sin \beta \sin ck_z] \quad (6)$$

$$\alpha_{2,4}(\mathbf{r}) = \frac{1}{2mr}[\mp k_F \sin \epsilon \cos \beta + k'_F \sin \beta \sin ck_z] \quad (7)$$

II. DENSITY OF STATES

In the semi-classical treatment, the argument of the Green's function $i\omega_n$ is replaced by $i\omega_n + \alpha$ where α is the Doppler shift. The quasiparticle energy is $E(\mathbf{k}) = \sqrt{\varepsilon^2(\mathbf{k}) + \Delta^2(\mathbf{k})}$ which is $\approx \sqrt{v_F^2 k_1^2 + v_g^2 k_2^2}$ in the vicinity of a node.¹⁹ Here k_1 points in the direction of the

node, k_2 is perpendicular to k_1 in the xy plane, and the gap velocity is $v_g = \partial\Delta/\partial k_2|_{\text{node}}$. In the vicinity of the j th node, the Green's function takes the form

$$G(\mathbf{k}, i\tilde{\omega}_n, \mathbf{r}) = \frac{i\tilde{\omega}_n + \alpha_j(\mathbf{r}) + v_F k_1}{(i\tilde{\omega}_n + \alpha_j(\mathbf{r}))^2 + v_F^2 k_1^2 + v_g^2 k_2^2} \quad (8)$$

where $i\tilde{\omega}_n = i\omega_n + i\Gamma_0$ and Γ_0 is the scattering rate at zero energy. The density of states is

$$N(\omega, \mathbf{r}) = -\frac{1}{\pi} \sum_{\mathbf{k}} \Im G(\mathbf{k}, \tilde{\omega}, \mathbf{r}). \quad (9)$$

We divide the volume of integration into four curved cylinder-shaped volumes, each centred around a line node on the Fermi surface¹⁹ and perform the integration across the disk spanned by k_1 and k_2

$$\begin{aligned} N(0, \mathbf{r}) &= \frac{\Gamma_0}{4\pi^3 v_F v_g} \sum_{j=1}^4 \int_{-\pi/c}^{\pi/c} dk_z \\ &\times \left[\ln \frac{p_0}{\sqrt{\alpha_j^2(\mathbf{r}) + \Gamma_0^2}} + \frac{\alpha_j(\mathbf{r})}{\Gamma_0} \tan^{-1} \frac{\alpha_j(\mathbf{r})}{\Gamma_0} \right] \end{aligned} \quad (10)$$

where p_0 is the integration cut-off. In the clean limit $|\alpha_j/\Gamma_0| \gg 1$ the density of states is

$$\begin{aligned} N(0, \mathbf{r}) &= \frac{1}{4\pi^3 v_F v_g} \int_{-\pi/c}^{\pi/c} dk_z (|\alpha_1(\mathbf{r})| + |\alpha_2(\mathbf{r})| \\ &+ |\alpha_3(\mathbf{r})| + |\alpha_4(\mathbf{r})|). \end{aligned} \quad (11)$$

Averaging over the vortex cross-section, we obtain

$$\begin{aligned} \langle N(0, \mathbf{r}) \rangle_H &= \frac{1}{4\pi^3 v_F v_g} \frac{1}{\pi R^2} \int_{\xi_0}^R dr r \int_0^{2\pi} d\beta \int_{-\pi/c}^{\pi/c} dk_z \\ &\times (|\alpha_1(\mathbf{r})| + |\alpha_2(\mathbf{r})| + |\alpha_3(\mathbf{r})| + |\alpha_4(\mathbf{r})|). \end{aligned} \quad (12)$$

This leads to the result

$$\begin{aligned} \langle N(0, \mathbf{r}) \rangle_H &\approx \frac{8}{\pi^3 v_g c \pi R} \left[\sqrt{b^2 + C^2} E \left(\frac{b^2}{b^2 + C^2} \right) \right. \\ &\left. + \sqrt{b^2 + S^2} E \left(\frac{b^2}{b^2 + S^2} \right) \right] \end{aligned} \quad (13)$$

where $b = v'_F/v_F$, c is the lattice constant in the c direction, $C = \cos \epsilon$, $S = \sin \epsilon$ and E is the complete elliptic integral of the second kind. Using $N_F \sim 1/cv_g\xi_0$ and $\xi_0/R \sim \sqrt{H/H_{c2}}$, we find

$$\begin{aligned} \langle N(0, \mathbf{r}) \rangle_H &\sim N_F \sqrt{\frac{H}{H_{c2}}} \left[\sqrt{b^2 + C^2} E \left(\frac{b^2}{b^2 + C^2} \right) \right. \\ &\left. + \sqrt{b^2 + S^2} E \left(\frac{b^2}{b^2 + S^2} \right) \right]. \end{aligned} \quad (14)$$

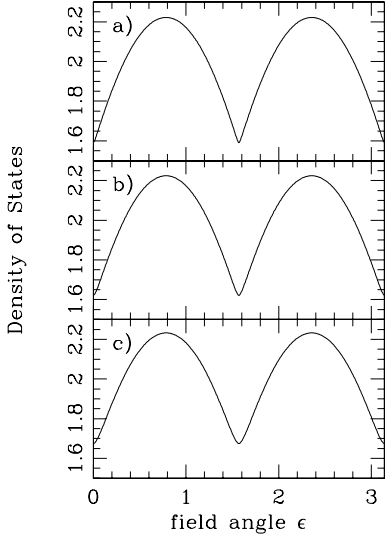


FIG. 2: Clean limit density of states (the dimensionless expression in the square brackets of Eq. 14) as a function of rotating field angle ϵ (in radians) for $b = 0.02, 0.05$ and 0.10 .

This function is shown in Fig. 2 for various values of b . It is seen that deviations from the perfectly 2D cylindrical Fermi surface leads to a softening of the cusps in the density of states.

In the dirty limit $|\alpha_j/\Gamma_0| \ll 1$ we get

$$\begin{aligned} \langle N(0, \mathbf{r}) \rangle_H &= \frac{\Gamma_0}{4\pi^3 v_F v_g} \frac{1}{\pi R^2} \int_{\xi_0}^R dr r \int_0^{2\pi} d\beta \int_{-\pi/c}^{\pi/c} dk_z \\ &\times \left(4 \ln \frac{p_0}{\Gamma_0} + \frac{\alpha_1^2(\mathbf{r})}{\Gamma_0^2} + \frac{\alpha_2^2(\mathbf{r})}{\Gamma_0^2} + \frac{\alpha_3^2(\mathbf{r})}{\Gamma_0^2} + \frac{\alpha_4^2(\mathbf{r})}{\Gamma_0^2} \right) \end{aligned} \quad (15)$$

which produces no oscillations with respect to the rotating field.

III. THERMAL CONDUCTIVITY

The thermal conductivity tensor is given by the Kubo formula, which is expressed in terms of the imaginary part of the Green's function as

$$\frac{\tilde{\kappa}(0, \mathbf{r})}{T} = \frac{k_B^2}{3} \sum_{\mathbf{k}} \mathbf{v}_F \mathbf{v}_F \text{Tr}[\Im \tilde{G}_{ret}(0, \mathbf{r}) \Im \tilde{G}_{ret}(0, \mathbf{r})], \quad (16)$$

where k_B is the Boltzmann constant and v_F is the Fermi velocity in the direction of \mathbf{k} . By again dividing the volume of integration into four regions and introducing the integration variable $p = \sqrt{v_F^2 k_1^2 + v_g^2 k_2^2}$ we find

$$\begin{aligned} \frac{\tilde{\kappa}(0, \mathbf{r})}{T} &= \frac{k_B^2}{3} \frac{1}{(2\pi^3) v_F v_g} \int_0^{2\pi} d\phi \int_0^{p_0} dp p \int_{-\pi/c}^{\pi/c} dk_z \\ &\times \sum_{j=1}^4 (\mathbf{v}_F \mathbf{v}_F)_j \frac{2\Gamma_0^2}{[(\alpha_j(\mathbf{r}) + p)^2 + \Gamma_0^2]^2} \quad (17) \\ &= \frac{k_B^2}{6\pi^2 v_F v_g} \int_{-\pi/c}^{\pi/c} dk_z \sum_{j=1}^4 (\mathbf{v}_F \mathbf{v}_F)_j \\ &\times \left(1 + \frac{\alpha_j(\mathbf{r})}{\Gamma_0} \left(\tan^{-1} \frac{\alpha_j(\mathbf{r})}{\Gamma_0} - \frac{\pi}{2} \right) \right) \quad (18) \end{aligned}$$

Using (2, 3), in zero magnetic field we get

$$\frac{\tilde{\kappa}(0, 0)}{T} = \frac{2k_B^2 v_F}{3\pi c v_g} \begin{pmatrix} 1 & 0 & 0 \\ 0 & 1 & 0 \\ 0 & 0 & (\frac{v'_F}{v_F})^2 \end{pmatrix}. \quad (19)$$

In a finite magnetic field, terms linear in the Doppler shift will vanish upon integration. So the magnetic part of the thermal conductivity is

$$\begin{aligned} \frac{\delta \tilde{\kappa}(0, \mathbf{r})}{T} &= \frac{k_B^2}{6\pi^2 v_F v_g} \int_{-\pi/c}^{\pi/c} dk_z \sum_{j=1}^4 (\mathbf{v}_F \mathbf{v}_F)_j \\ &\frac{\alpha_j(\mathbf{r})}{\Gamma_0} \tan^{-1} \frac{\alpha_j(\mathbf{r})}{\Gamma_0} \end{aligned} \quad (20)$$

In the clean limit, this reduces to

$$\frac{\delta \tilde{\kappa}(0, \mathbf{r})}{T} = \frac{k_B^2}{12\pi v_F v_g} \int_{-\pi/c}^{\pi/c} dk_z \sum_{j=1}^4 (\mathbf{v}_F \mathbf{v}_F)_j \frac{|\alpha_j(\mathbf{r})|}{\Gamma_0}. \quad (21)$$

The integrand is

$$\frac{v_F^2}{\Gamma_0} \begin{pmatrix} |\alpha_2| + |\alpha_4| & 0 & \frac{v'_F}{v_F} (|\alpha_2| - |\alpha_4|) \sin ck_z \\ 0 & |\alpha_1| + |\alpha_3| & \frac{v'_F}{v_F} (|\alpha_1| - |\alpha_3|) \\ \frac{v'_F}{v_F} (|\alpha_2| - |\alpha_4|) \sin ck_z & \frac{v'_F}{v_F} (|\alpha_1| - |\alpha_3|) \sin ck_z & (\frac{v'_F}{v_F})^2 (|\alpha_1| + |\alpha_2| + |\alpha_3| + |\alpha_4|) \sin^2 ck_z \end{pmatrix}. \quad (22)$$

The off-diagonal components vanish in the vortex average, and the diagonal components are

$$\frac{\langle \delta \kappa_{xx} \rangle_H}{T} = \frac{4}{3\pi^2} \frac{k_B^2}{R\Gamma_0} \frac{v_F^2}{v_g c} \sqrt{b^2 + S^2} E \left(\frac{b^2}{b^2 + S^2} \right) \quad (23)$$

$$\frac{\langle \delta \kappa_{yy} \rangle_H}{T} = \frac{4}{3\pi^2} \frac{k_B^2}{R\Gamma_0} \frac{v_F^2}{v_g c} \sqrt{b^2 + C^2} E \left(\frac{b^2}{b^2 + C^2} \right) \quad (24)$$

$$\begin{aligned} \frac{\langle \delta \kappa_{zz} \rangle_H}{T} = & \frac{4}{9\pi^2} \frac{k_B^2}{R\Gamma_0} \frac{v_F^2}{v_g c} \left(\sqrt{b^2 + S^2} \left[-S^2 K \left(\frac{b^2}{S^2 + b^2} \right) \right. \right. \\ & \left. \left. + (2b^2 + S^2) E \left(\frac{b^2}{S^2 + b^2} \right) \right] \right. \\ & \left. + \sqrt{b^2 + C^2} \left[-C^2 K \left(\frac{b^2}{C^2 + b^2} \right) \right. \right. \\ & \left. \left. + (2b^2 + C^2) E \left(\frac{b^2}{C^2 + b^2} \right) \right] \right) \quad (25) \end{aligned}$$

where K is the complete elliptic integral of the first kind. κ_{zz} is plotted in Fig. 3 for different values of b . In the limit $b \rightarrow 0$ the cusps are sharp, however the oscillation amplitude goes to zero. The oscillation amplitude increases exponentially with b .

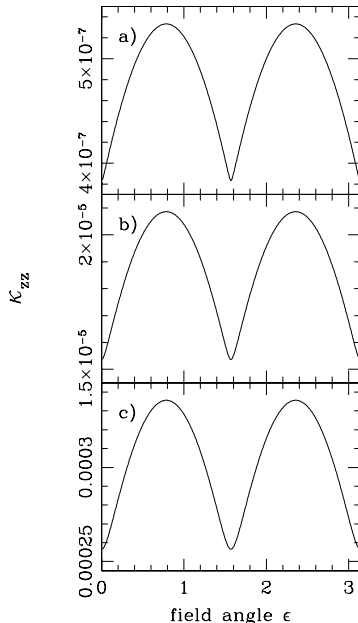


FIG. 3: Clean limit thermal conductivity κ_{zz} (the dimensional expression in the round brackets of Eq. 25) as a function of rotating field angle ϵ (in radians) for $b = 0.02, 0.05$ and 0.10 .

In the dirty limit, (20) reduces to

$$\frac{\delta \tilde{\kappa}(0, \mathbf{r})}{T} = \frac{k_B^2}{6\pi^2 v_F v_g} \int_{-\pi/c}^{\pi/c} dk_z \sum_{j=1}^4 (\mathbf{v}_F \mathbf{v}_F)_j \frac{\alpha_j^2(\mathbf{r})}{\Gamma_0^2} \quad (26)$$

Again, the off-diagonal components vanish in the vortex average, and the diagonal elements are

$$\left\langle \frac{\delta \kappa_{xx}(0, \mathbf{r})}{T} \right\rangle_H = \frac{k_B^2 v_F^3}{12\pi v_g} \log(R/\xi_0) (2C^2 + b^2) \quad (27)$$

$$\left\langle \frac{\delta \kappa_{yy}(0, \mathbf{r})}{T} \right\rangle_H = \frac{k_B^2 v_F^3}{12\pi v_g} \log(R/\xi_0) (2S^2 + b^2) \quad (28)$$

$$\left\langle \frac{\delta \kappa_{zz}(0, \mathbf{r})}{T} \right\rangle_H = \frac{k_B^2 v_F^3}{12\pi v_g} \log(R/\xi_0) (1 + 3b^2/2) \quad (29)$$

Similar to the dirty limit density of states (15), there are no rotating field-dependent oscillations in the dirty limit of κ_{zz} .

IV. DISCUSSION AND CONCLUSIONS

The topology of the true Fermi surface of $\text{YNi}_2\text{B}_2\text{C}$ shown in Ref. 15 is difficult to discern, however the validity of our calculation only requires that the Fermi surface exists at the positions of the nodes and spans all or most of the Brillouin zone in the c direction with a slight curvature characterised by the parameter b . The main point is that the cusp features observed in the field angle-dependent heat capacity¹⁰ are a feature of *line nodes* and the cusp features observed in the field angle-dependent thermal conductivity are a feature of *line nodes on a quasi-2D Fermi surface*. In contrast, the semi-classical (Doppler shift) treatment of point nodes (which may not even be valid) is insensitive to Fermi surface topology and produces neither cusp features *nor* four-fold oscillations.¹⁸

Using $R \approx 4 \times 10^{-8}$ m (for a 1 T field), $T = 0.56$ K, $E_F = 9$ Ry,¹⁵ $v_F \approx 3 \times 10^7$ m/s, gap maximum $\Delta_0 = v_g \hbar k_F = 30$ K and scattering rate $\Gamma_0 = 1$ K leads to an estimate of the prefactor in (25) of $\frac{4T}{9\pi^2} \frac{k_B^2}{R\Gamma_0} \frac{v_F^2}{v_g c} \approx 10^4$ W/Km. The experimentally observed oscillation amplitude is $\approx 2 \times 10^{-3}$. Comparing with the oscillation amplitudes shown in Fig. 3, one may deduce that the value of b is approximately 0.02. Such a small value of b produces sharp cusps in the field angle-dependent κ_{zz} oscillations and is therefore fully consistent with experiment.

Thus the most straight-forward model that best describes accumulated observations on $\text{YNi}_2\text{B}_2\text{C}$ is that the superconducting order parameter is $\Delta \sim k_x k_y$, which belongs to the irreducible representation B_{2g} of the point group D_{4h} , with associated line nodes along $k_x = 0$ and $k_y = 0$.

-
- ¹ K. Izawa, K. Kamata, Y. Nakajima, Y. Matsuda, T. Watanabe, M. Nohara, H. Takagi, P. Thalmeier and K. Maki, *Phys. Rev. Lett.* **89**, 137006 (2002).
 - ² R. J. Cava, H. Takagi, H. W. Zandbergen, J. J. Krajewski, W. F. Peck Jr., T. Sigríst, B. Batlogg, R. B. van Dover, R. J. Felder, K. Mizuhashi, J. O. Lee, H. Eisaki and S. Uchida, *Nature* **367**, 252 (1994).
 - ³ C. Godart, L. C. Gupta, R. Nagarajan, S. K. Dhar, H. Noel, M. Potel, C. Mazumdar, Z. Hossain, C. Levy-Clement, G. Schiffmacher, B. D. Padalia and R. Vijayaraghavan, *Phys. Rev. B* **51**, 489 (1995).
 - ⁴ M. Nohara, M. Isshiki, F. Sakai and H. Takagi, *J. Phys. Soc. Jpn.* **68**, 1078 (1999); M. Nohara, H. Suzuki, N. Mangkorntong and H. Takagi, *Physica C* **341-348**, 2177 (2000).
 - ⁵ K. Izawa, H. Yamaguchi, Y. Matsuda, H. Shishido, R. Settai and Y. Onuki, *Phys. Rev. Lett.* **87**, 057002 (2001).
 - ⁶ G.-Q. Zheng, Y. Wada, K. Hashimoto, Y. Kitaoka, K. Asayama, H. Takeya and K. Kadowaki, *J. Phys. Chem. Solids* **59**, 2169 (1998).
 - ⁷ I.-S. Yang, M. V. Klein, S. L. Cooper, P. C. Canfield, B. K. Cho and S.-I. Lee, *Phys. Rev. B* **62**, 1291 (2000).
 - ⁸ G. E. Volovik and L. P. Gor'kov, *Sov. Phys. JETP* **61**, 843 (1985).
 - ⁹ M. Sigríst and K. Ueda, *Rev. Mod. Phys.* **63**, 239 (1991).
 - ¹⁰ T. Park, M. B. Salamon, E. M. Choi, H. J. Kim and S.-I. Lee, *Phys. Rev. Lett.* **90**, 177001 (2003).
 - ¹¹ Y. Matsuda, K. Izawa and I. Vekhter, *J. Phys.: Condens. Matter* **18**, R705 (2006).
 - ¹² T. Sigríst, *Nature* **367**, 254 (1994).
 - ¹³ J. I. Lee, T. S. Zhao, I. G. Kim, B. I. Min and S. J. Youn, *Phys. Rev. B* **50**, 4030 (1994).
 - ¹⁴ D. J. Singh, *Solid State Commun.* **98**, 899 (1996).
 - ¹⁵ K. Yamaguchi, H. Katayama-Yoshida, A. Yanase and H. Harima, *Physica C* **412-414**, 225 (2004).
 - ¹⁶ G. E. Volovik, *JETP Lett.* **58**, 471 (1993).
 - ¹⁷ H. Aubin, K. Behnia, M. Ribault, R. Gagnon and L. Taillefer, *Phys. Rev. Lett.* **78**, 2624 (1997).
 - ¹⁸ T. R. Abu Alrub and S. H. Curnoe, *Phys. Rev. B* **78**, 104521 (2008).
 - ¹⁹ A. C. Durst and P. A. Lee, *Phys. Rev. B* **62**, 1270 (2000).